



*Full Length Research Paper*

## In-situ Observation of Retained Austenite and Residual Stress Evolutions during Tempering of carbonitrided DIN 1.6587 Alloy Steel

Richard J. Katemi<sup>1\*</sup> and Jérémy Epp<sup>2,3</sup>

<sup>1</sup>University of Dar es Salaam, Chemical and Mining Engineering Department, P.O. Box 35131, Dar es Salaam, TANZANIA

<sup>2</sup> Leibniz-Institute for Materials Engineering-IWT Bremen, Badgasteiner str. 3, 28359 Bremen, GERMANY

<sup>3</sup> MAPEX Center for Materials and Processing, University of Bremen, Badgasteiner Str. 3, 28359 Bremen, GERMANY

\*Corresponding author: rkatemi@gmail.com

### ABSTRACT

This paper investigates the evolution of retained austenite and residual stresses during and after tempering of carbonitrided 18CrNiMo7-6 low alloy steel carried out using in-situ X-ray diffraction technique. In this case, two carbonitriding treatments with different surface the retained austenite contents of 20 and 54 mass.-% are investigated. The tempering is carried out in a continuous heating mode to 650°C as well as in isothermal mode at holding temperature of 170, 240, and 300°C for 2 hours. During continuous heating at a heating rate of 10°C/min, the retained austenite started to decompose at 290°C. On isothermal holding at 170°C for 2 hours, the retained austenite remained relatively stable at 20 and 54 mass.-% while readily decomposed to less than 5 mass.-% on holding at 300°C. On continuous heating, residual stress in martensite continuously relaxes and reaches full relaxation (0 MPa) at about 400°C. During isothermal holding, residual stresses in martensite are increasingly relaxed with increasing holding tempering. Further relaxation of residual stresses is observed during cooling whereas a cyclic variation of the residual stresses in the retained austenite could be determined.

### ARTICLE INFO

Submitted: May 5, 2022

Revised: June 15, 2022

Accepted: June 26, 2022

Published: June 30, 2022

**Keywords:** Carbonitriding, retained austenite, residual stresses, tempering, and in-situ XRD

### INTRODUCTION

Carbonitriding is a thermochemical process during which the treated component is enriched simultaneously with carbon and nitrogen interstitial atoms in austenitic field. Researches in the last decade have focused on carbonitriding atmosphere (Hoffmann et.al, 2011; Okhi, 2006) aiming at controlling independently the carbon and nitrogen potentials. Controlling carbon and nitrogen potentials allows adjusting the

surface carbon and nitrogen content to the target values which is essential to achieve the desired product properties and reliability (Hoffmann et. al, 2011).

The presence of nitrogen in the case carbonitrided layer improves hardenability of low alloy steels and wear resistance as well as a high temperature stability of the treated parts (Winter, 2011). Furthermore, nitrogen stabilizes austenite and enables retaining up to 50 mass.-% of austenite after

quenching. Such high amount of retained austenite influences not only the mechanical properties but also the magnitudes and distribution of residual stresses in both martensite and retained austenite in the case hardened layer (Katemi et. al, 2014). The thermal stability of such retained austenite is a key to avoiding distortion that might occur while component is in service. In some cases treated components are temporarily subjected to an elevated temperature in excess of 400°C; for example during galvanizing in a molten zinc-rich alloy (Lonardelli et. al, 2012). It is possible that at such high temperature retained austenite may not be sufficiently thermally stable leading to decomposition into thermodynamic stable microstructure of ferrite and cementite and therefore strongly reduced mechanical properties. However, to date very limited information is available describing the influence of the tempering process on the thermal stability of retained austenite and the residual stress in carbonitrided components. Furthermore, nearly all available information on stability of retained austenite pertain to carburized or

medium plain carbon parts containing only carbon atoms in interstitial sites (Lonardelli et.al, 2012).

In this work the thermal stability of retained austenite and residual stresses during tempering of carbonitrided samples was investigated using DIN 1.6587 alloy steel. Two carbonitriding treatments with different surface carbon and nitrogen contents were used. The investigation was carried using in-situ X-ray diffraction which enables following the microstructural evolution like of phase fractions, lattice parameters and residual stresses during continuous heating and isothermal holding.

## METHODS AND MATERIALS

### Material

The initial chemical composition of DIN 1.6587 alloy steel is given in Table 1 with pearlite + ferrite initial microstructures. Samples with a diameter of 22 mm and thickness 2 mm were prepared then subjected to carbonitriding treatment.

**Table 1:** Chemical composition of DIN 1.6587 alloy steel

Element	C	Cr	Ni	Mn	Mo	Si	Al	S	Fe
Content [mass.-%]	0.157	1.65	1.57	0.517	0.259	0.269	0.022	0.028	Bal

### Carbonitriding treatment

Two carbonitriding treatments designated as CN1 and CN2 were used in order to generate microstructures with different fractions of retained austenite and martensite phase. For CN1, the target carbon and nitrogen surface content was 0.6 and 0.4 mass.-% whereas for CN2 the targets were 0.87 and 0.34 mass.-%, respectively. The details of the carbonitriding treatment have been presented in previous work of the authors (Katemi and Epp, 2019). Hardening was accomplished by quenching into oil held at 60°C. In the as-quenched state, the samples consisted of supersaturated

martensite and retained austenite phase and were subjected to further treatment in this state. Finally, after rinsing in water held at 70°C the samples were electro-polished to remove oxidized layer without introducing new residual stresses or inducing phase transformations. The electro-polishing was carried out using an electrolyte solution containing 80% H<sub>3</sub>PO<sub>4</sub> and 20% H<sub>2</sub>SO<sub>4</sub> and a layer of about 50 µm was removed.

### Tempering cycles

In the first place, in situ experiments were performed to establish the temperature range of retained austenite stability. For this, a continuous heating from room

temperature (RT) to 650 °C at a slow heating rate of 10 °C/min was used. After establishing the range of stability during continuous heating, in situ tempering experiments were carried out considering different typical temperature-time cycles. In each case, the complete tempering cycle comprised a heating at 10 °C/min from RT to the holding temperature, isothermally holding at this temperature for 2 hours then cooling at 10 K/min to RT. The holding temperatures employed were 170°C, 240°C, and 300 °C. A K-type thermocouple was used to control the temperature using Eurotherm™ temperature controller. For each tempering cycle, two experiments were conducted and the results were averaged; the results were reproducible. In order to avoid sample oxidation, a secondary vacuum of about  $10^{-3}$  mbar was created in the furnace chamber followed by purging with nitrogen gas at a rate of 0.5 litre/second throughout the experiment.

### X-ray diffraction

The in-situ X-ray diffraction measurements were performed using a Bruker AXS D8 diffractometer (Figure 1) equipped with a position sensitive detector (Vantec-1) with high resolution and a Cr ( $\lambda_{\alpha_1}=2.28975 \text{ \AA}$ ) rotating anode. The operating conditions were selected to enable rapid acquisition of data with high quality. In this case, an anode current of 300 mA and a voltage of 33 kV were used.

For phase analysis, the scanning range was from 62 to 132° 2 $\theta$  with a scan step of 0.11° 2 $\theta$ . The X-ray diffraction patterns collected were analysed using the Rietveld Method (software Topas 4.2, Bruker Axs) (Young, 1993) using a fundamental parameter refinement approach. A NIST LaB<sub>6</sub> reference powder was measured to determine the instrumental contribution on the diffraction patterns. The analysis of these diffraction patterns yielded the phase fraction of retained austenite and martensite/ferrite and their respective lattice parameters.

For residual stress analysis,  $\omega$ -mode was used, where the tilt angle ( $\psi$ ) is defined by  $\psi=2\theta/2-\omega$  with  $\omega$  the rotation of the sample in the diffractometer. For retained austenite the {220} peak was measured with a scanning range from 122° to 132° 2 $\theta$  using a scan step of 0.07° 2 $\theta$ . For martensite phase, {211} peak was measured with a scanning range from 148 to 158° 2 $\theta$  and a scan step of 0.12° 2 $\theta$ . The  $\omega$ -angles and their corresponding Psi ( $\psi$ ) angles used for residual stress measurements in retained austenite and martensite phase are given in Table 2.

The collected diffraction patterns for both  $\gamma$ -{220} and  $\alpha'$ -{211} lines were analyzed using a DIFFRAC<sup>plus</sup> STRESS (Bruker-AXS) using the sliding gravity method. The sliding gravity thresholds used were 30, 40, 50, 60 and 70% of the maximum intensity after linear background subtraction.

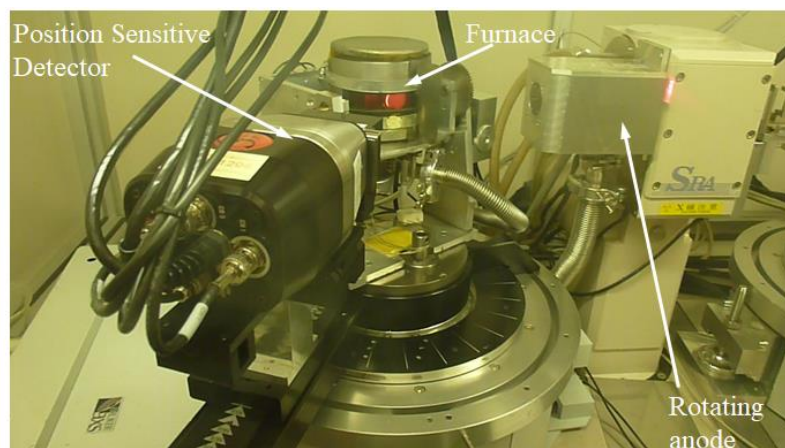


Figure 1: Bruker AXS D8 diffractometer

**Table 2:**  $\omega^\circ$  and Psi ( $\psi^\circ$ ) angles for austenite and martensite phase

Retained austenite {220}		Martensite {211}	
$\omega^\circ$	Corresponding Psi ( $\psi^\circ$ )	$\omega^\circ$	Corresponding Psi ( $\psi^\circ$ )
21.5	-42.0	34.5	-43.5
35.5	-28.0	48.7	-29.4
49.9	-13.7	62.8	-15.2
63.5	0.0	76.5	-1.22
78.2	14.7	91.2	13.1
92.4	28.8	105.3	27.3
106.5	43	119.5	41.5

The dependence of X-ray elastic constants on temperature for both retained austenite and martensite phases were calculated based on the temperature dependent macroscopic elastic properties given by Richter (Richter, 1983). For martensite phase, the Poisson's ratio and Young's modulus dependence on temperature were defined as:

$$\nu^{(211)} = 0.0283 + 4 \times 10^{-10} T \quad (1)$$

$$E^{(211)} = [214 - 5.2 \times 10^{-2} T - 4.7 \times 10^{-4} T^2] \times 1000 [MPa] \quad (2)$$

On the other hand, the X-ray constants for retained austenite were collected as in (3) and (4):

$$\nu^{(211)} = 0.292 + 5.4 \times 10^{-5} T \quad (3)$$

$$s_1 = - \left( \frac{\nu_T^{\{220\}}}{E_T^{\{220\}}} \right) + 0.0279503 \left( \frac{\nu_T^{\{220\}} + 1}{E_T^{\{220\}}} \right) \quad (7)$$

$$\frac{1}{2} s_2 = 0.916149 \left( \frac{\nu_T^{\{220\}} + 1}{E_T^{\{220\}}} \right) \quad (8)$$

## RESULTS AND ANALYSIS

### Carbon and nitrogen content after carbonitriding

The carbon and nitrogen depth profiles of the as-quenched specimens for both CN1 and CN2 conditions are shown in Figure 2. In all cases the effective case depth (CHD) was 1 mm. The maximum carbon and

$$E^{(200)} = [200 - 8.3 \times 10^{-2} T] \times 1000 \text{ MPa} \quad (4)$$

whereas the evolution of the specific elastic constants ( $s_1$  and  $1/2s_2$ ) for the diffracting planes hkl were estimated according to the following expressions (Richter, 1983):

For martensite:

$$s_1 = - \left( \frac{\nu_T^{\{211\}}}{E_T^{\{211\}}} \right) + 0.020488 \left( \frac{\nu_T^{\{211\}} + 1}{E_T^{\{211\}}} \right) \quad (5)$$

$$\frac{1}{2} s_2 = 0.938545 \left( \frac{\nu_T^{\{211\}} + 1}{E_T^{\{211\}}} \right) \quad (6)$$

For retained austenite is expressed by (7) and (8) as:

nitrogen content at a depth of 50  $\mu\text{m}$  are 0.58 and 0.28 mass.-% for CN1 and 0.86 and 0.47 mass.-% for CN2, respectively. The maximum amount of retained austenite was determined at 50  $\mu\text{m}$  below the surface directly after quenching by analyzing room temperature X-ray diffraction patterns: 18 mass.-% for CN1 and 54 mass.-% for CN2.

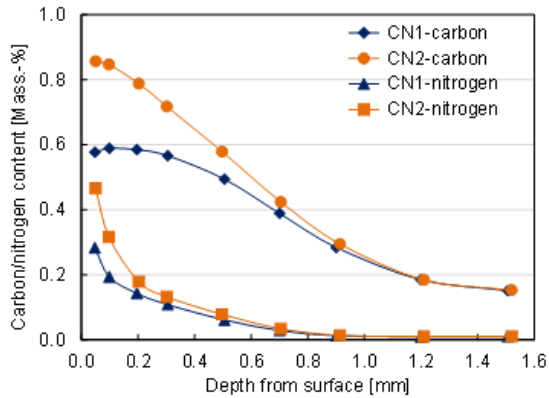


**Figure 2: Carbon and nitrogen depth profiles after carbonitriding treatment**

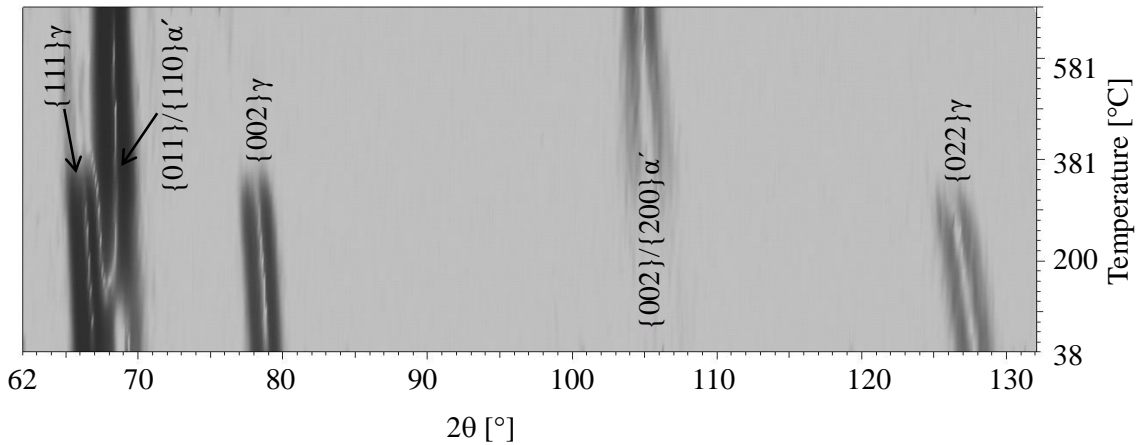
### Evolution of phase fractions during tempering

Figure 3 presents 2D top-view plot of all measured diffraction patterns showing the peak positions as a function of the temperature during continuous heating to 650 °C at a heating rate of 10 °C/min for condition CN2. The initial room temperature state exhibits strong austenite (Fe- $\gamma$ ) and broad martensitic ( $\alpha'$ ) reflections. Peaks of finely disseminated precipitates could not be detected by XRD in this state. As can be seen from this figure, the intensity of retained austenite peaks  $\gamma\{111\}$ ,  $\gamma\{002\}$  and  $\gamma\{022\}$  start to disappear at around 250 °C and decrease continuously until these have disappeared completely meanwhile the intensity martensite peaks  $\alpha'\{011\}/\{110\}$  and  $\alpha'\{002\}/\{200\}$  increases and the peaks get narrower. The shift in  $2\theta$  reflects different effects on the lattice parameters of the phases.

Analysis of the diffraction patterns collected during continuous heating gives the temperature range of thermal stability

of retained austenite as shown in Figure 4. In both CN1 and CN2 a slight increase in RA between 110° and 170 °C is observed, which is in the range of the uncertainties associated with these evaluations. In this temperature range redistribution of carbon and nitrogen through homogenisation and precipitation of transition carbides and  $\alpha''$ -Fe<sub>16</sub>N<sub>2</sub> nitrides takes place, leading to a decrease in martensite integral intensity, rather than growth of austenite. This influences the evaluation using the Rietveld Method, since the very small peaks from the precipitates cannot be distinguished due to the fast measurements.

As can be seen in Figure 4a and b, the RA present at RT is stable up to about 290 °C. Above this temperature, RA starts to decompose and the maximum decomposition rate occurs at 350 °C. At 400 °C, the amount of RA present in the samples is about 3.5 and 8 mass.-% for CN1 and CN2, respectively. Upon further heating, small amount of RA is still present which continues to decompose and reaches 0 and 4 mass.-% for CN1 and CN2 at 650 °C. Although the starting temperature of RA decomposition (above 290 °C) is in good agreement with that observed in the work of Amarthalingam (Kannengiesser et.al, 2010) it is highly affected by the heating rate as well as the type and content of alloying elements that stabilize or destabilize austenite. The increasing the vanadium amount up 4 mass-% leads to extended stability range but is shifted to lower temperatures while at 8 mass-% Chromium retained austenite is very stable and decomposes only above 400°C.



**Figure 3:** 2D plot showing top view of diffraction patterns as a function of temperature during continuous heating of CN2 sample up to 650 °C.

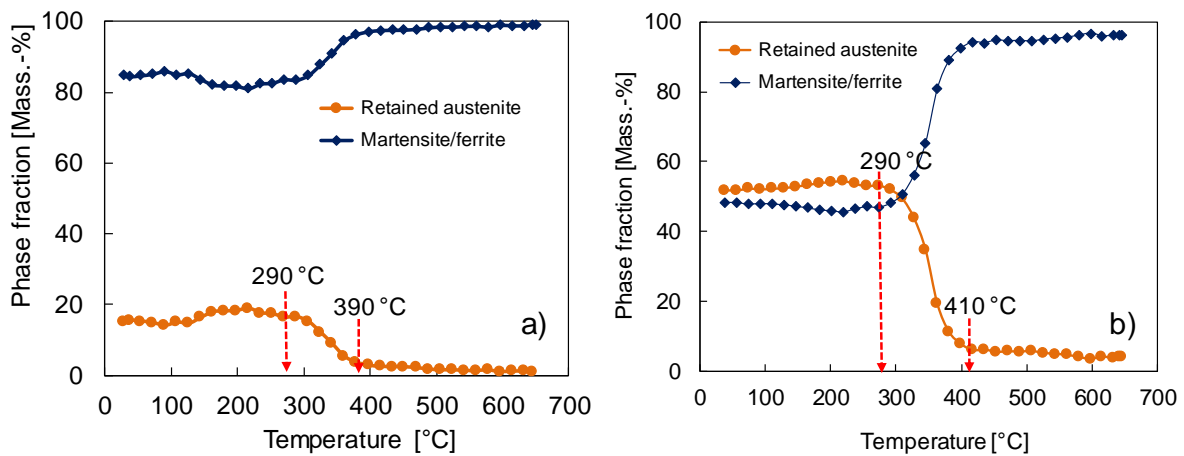


**Figure 4:** Evolution of retained austenite and martensite contents during continuous heating: (a) CN1 with 0.6 %C and 0.4 %N at a depth of 50 μm; (b) CN2 with 0.87 %C and 0.34 %N at a depth of 50 μm

Figure 5 illustrates the effect of tempering temperature on the stability of retained austenite during a typical complete isothermal tempering cycle. In all cases, the heating and cooling rates were 10 K/min whereas the holding temperatures were 170°C, 240°C and 300 °C for 2 hours. It can be seen that the initial amounts of retained austenite at room temperature correspond to those observed in Figure 4 reflecting the reproducibility in carbon and nitrogen content after carbonitriding treatment. As expected, the decomposition rate of retained austenite increases with holding temperature. During tempering at 170 °C for 2 hours (Figure 4), retained austenite remains rather stable for both conditions and no austenite transformation

occurred even during the subsequent cooling. At 240 °C (Figure 4b), a moderate but continuous transformation of retained austenite is observed during the whole holding and cooling steps. Holding at 300 °C (Figure 4c) leads to rapid decomposition of the austenite with less than 5 mass-% austenite for both conditions after the process.

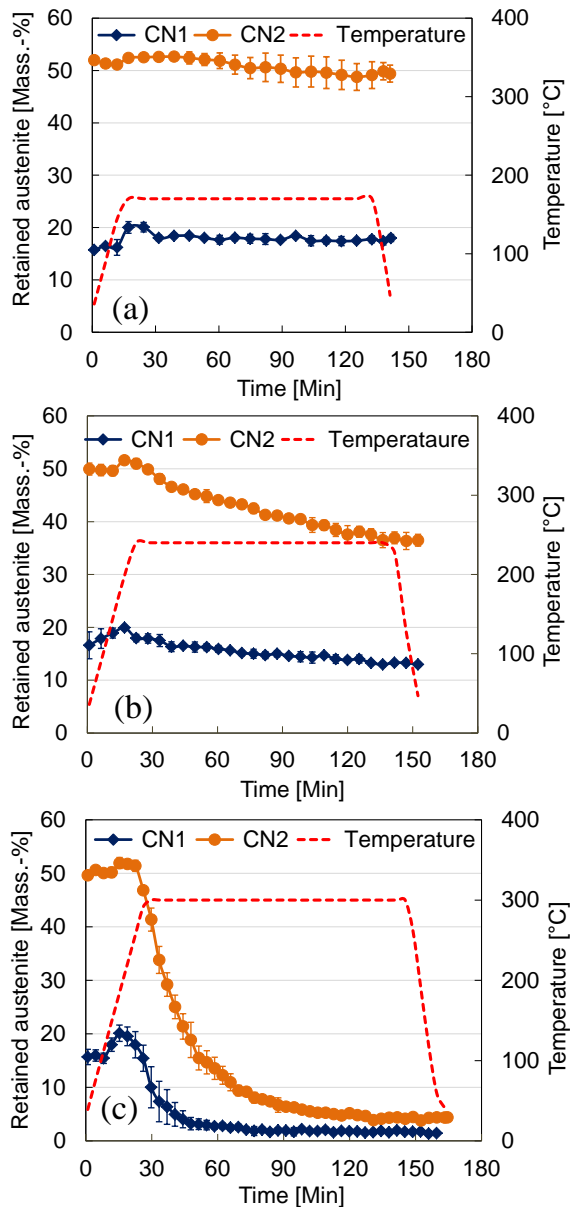


**Figure 5: Time dependent evolution of retained austenite content for CN1 and CN2 during tempering with isothermal holding for 2 hours at different temperatures: a) 170 °C, b) 240 °C, c) 300 °C**

### Evolution of residual stresses

The evolution of residual stresses in retained austenite and martensite for CN1 and CN2 treatments during continuous heating to 650 °C is shown in Figure 6. It has to be noted that in all cases, the measurements were done at a depth of about 50  $\mu\text{m}$  from the surface which is characterized by the maximum amount of retained austenite; hence less compressive compressive residual stresses in martensite

phase. Analysis of the diffraction patterns collected at room temperature reveals retained austenite to be slightly in tension with initial residual stresses of 0 MPa for CN1 and +33 MPa for CN2 whereas martensite is slightly in compression with -65 MPa for CN1 and -233 MPa for CN2. The differences in initial residual stresses between the two treatments can mainly be due to the differences in the initial martensite and retained austenite proportions (18 and 54 mass.-% RA for CN1 and CN2, respectively) while the low magnitude of residual stresses may be attributed to small thickness of the samples (i.e 2 mm thick) and through-carbo-nitriding.

As can be seen from Figure 6, martensite and retained austenite respond differently at different temperatures. The compressive residual stresses in martensite phase for both treatments CN1 and CN2 relax continuously with increasing temperature. Full residual stress relaxation ( $\sigma \approx 0$  MPa) is reached between 350°C and 400°C. The stress relaxation is associated to re-organization of thermally activated dislocations as well as diffusion of interstitial carbon and nitrogen atoms toward the area of high dislocation density and grain boundaries (Mittemeijer, 1986). Beyond 400°C, the residual stresses in martensite remains relatively zero. On the other hand, the evolution of residual stresses in retained austenite during continuous heating exhibits a cyclic behaviour. Retained austenite associated with the martensite exists as irregular volumes between martensite plates in the high-carbon regions of the case. This is linked to the changes in chemical composition occurring in both retained austenite and martensite. The evolution of martensite due to clustering and formation of  $\epsilon/\eta$  – precipitates as well as the loss of martensite tetragonality lead to the change in specific volume play an important role on the variation of residual stresses in retained austenite as a function of temperature.

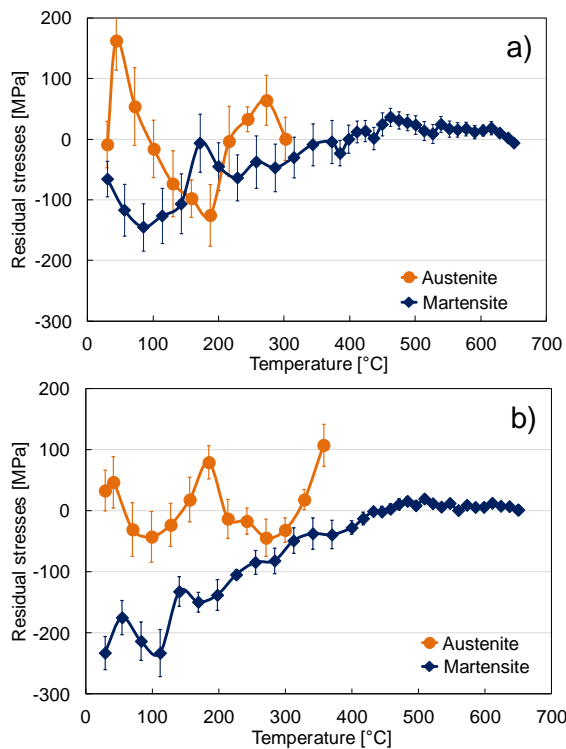


**Figure 6: Evolution of residual stresses in austenite and martensite during continuous heating from RT to 650 °C at a heating rate of 10 K/min: a) CN1, b) CN2.**

The residual stress evolutions during isothermal tempering cycles are shown in Figure 7. For isothermal holding at 240 °C and 300 °C, measurement of residual stresses in retained austenite was mainly conducted during heating and partly during holding due to low intensity of retained austenite as its amount falls below 15 mass.-%, making precise fast measurements difficult. For both CN1 and CN2 treatments, the initial residual stresses in martensite phase range from -100 to -250 MPa. The difference in initial magnitude of residual stresses may be attributed to scatter from one sample to another for the martensite to retained austenite ratio, the

depth at which the measurements were conducted ( $50 \pm 10 \mu\text{m}$ ), the effective case depth as well as level of carbon+nitrogen reached after carbonitriding process.

In all cases a considerable residual stress relaxation in martensite phase occurs mainly during heating to the holding temperature, but also in the final cooling to RT, in particular for CN2. As already discussed for continuous heating, the relaxation of residual stresses is associated to re-organization of thermally activated dislocations as well as movement of interstitial carbon and nitrogen atoms toward the area of high dislocation density and grain boundaries (Mittemeijer, 1986).

Although the residual stresses for CN1 (Figures 7a, c and d) remain rather constant during the holding step, the magnitude of compressive residual stresses decreases with increasing holding temperature and is about -75, -65, and -30 MPa during isothermal holding temperature at 170°C, 240°C, and 300°C, respectively. Similarly, for CN2 residual stresses decreases mainly during the heating stage. Contrarily to CN1, the increasing tempering temperature does not seem to affect strongly the remaining compressive stresses which are in a range between -80 and -120 MPa during holding. On the other hand, it is interesting to remark that further residual stress relaxation takes place in martensite as well as in retained austenite during cooling to RT after holding. This behaviour might be attributed to plastic deformation of the core leading to the decrease of mismatch between the surface and the core during cooling stage. Such behaviour is obviously present when still high amount of retained austenite is present during cooling.

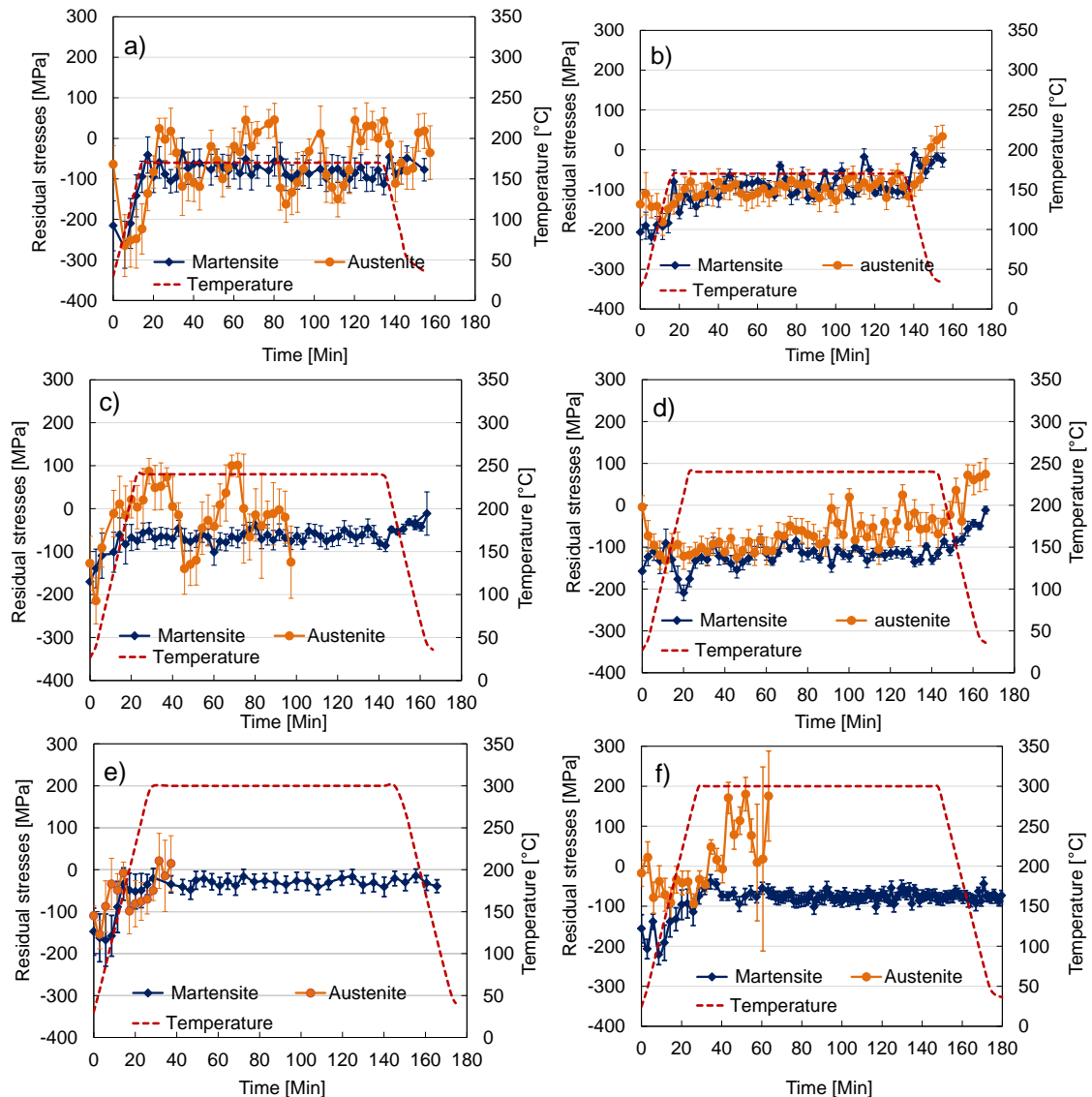


**Figure 7: Effect of tempering cycles on the evolution of residual stresses in carbonitrided specimens for different isothermal holding temperatures: a), c) and e) at 170/240/300 °C for CN1; b), d) and f) at 170/240/300 °C for CN2, respectively.**

## CONCLUSION

This work investigated the evolution of retained austenite and residual stresses during continuous and isothermal holding of carbonitrided DIN 1.6587 alloy steel. After carbonitriding, the as-quenched retained austenite was 18 and 54 mass.-% for CN1 and CN2, respectively. On continuous heating, retained austenite remained relatively stable until 290 °C and readily decomposed to reach zero and 4 mass.-% at 650 °C for CN1 and CN2, respectively. On isothermal holding at 170 °C, retained austenite remained stable whereas at 300 °C decomposed rapidly to

reach <5 mass.-% after 2 hours. Further residual stress relaxation takes place in martensite as well as in retained austenite during cooling to RT after holding.

As-quenched martensite was in compression -65 and -233 MPa for CN1 and CN2, respectively. During continuous heating, residual stresses in martensite continuously relaxed and reached full relaxation at about 400 °C whereas retained austenite exhibited a cyclic variation. On isothermal holding, although residual stresses for CN1 remained constant the magnitude of compressive residual stresses decreased with increasing

holding temperature and is about -75, -65, and -30 MPa for isothermal holding temperature at 170°C, 240°C, and 300°C, respectively. For CN2, isothermal residual stresses remained between -80 MPa and -120 MPa. Furthermore, residual stress relaxation in both martensite and retained austenite phase was observed during cooling to room temperature.

## REFERENCE

- Cheng L., Böttger A., Mittemeijer E.M. (1992), Tempering of iron-carbon-nitrogen martensites, *Metallurgical Transaction A*, 23(A): 1129-1145.
- Epp J. (2017), Effects of Hydrostatic 2nd Kind Residual Stresses and of Carbon Partitioning During Martensitic Quenching of Low Alloy Steel, *Materials Research Proceedings*, 2: 283-288.
- Hoffmann F.T., Matthias S., Clausen B., Bischoff S., Klumper-Westkamp (2011), New Carbonitriding Processes. Proc. 26<sup>th</sup> Heat Treating Society Conference, Detroit, USA :115-121.
- Kannengiesser T., Babu S.S., Komizo Y-I., Ramirez A.J. (Eds) (2010), *In-situ studies with photon, neutron and electrons scattering*, Springer, Berlin: 133-148
- Katemi R.J. and Epp J. (2019), Influence of tempering and cryogenic treatment on retained austenite and residual stresses in carbonitrided 18CrNiMo7-6 Low Alloy Steel, *Tanzania Journal of Engineering and Technology*, 38(1): 71-82.
- Katemi R.J., Epp J., Hoffmann F.T, Steinbacher M. (2014), Investigations of residual stress distributions in retained austenite and martensite after carbonitriding of a low alloy steel, *Advanced Materials Research.*, 996: 550-555.
- Lonardelli I., Peet M., Van Beek W., Bhadeshia H.K.D.H. (2012), Powder metallurgical nanostructured medium carbon bainitic steel: kinetics, structure, and in-situ thermal stability studies, *Material Science and Engineering A*, 555: 139-147.
- Mittemeijer E.J., van Gent A., van der Schaaf P.J. (1986), Analysis of transformation kinetics by nonisothermal dilatometry, *Metall. Trans. A*, 17(A): 1441-1445.
- Okhi C. (2006), Atmospheric Control Method for JIS-SUJ2 Carbonitriding Processes, *NTN Technical Review No. 74*: 44-53.
- Onink M., Brakman C.M., Tichelaar F.D., Mittemeijer E.M., van der Zwaag S., Root J.H., Konyer N.B. (1993), The lattice parameters of austenite and ferrite in Fe-C alloys as functions of carbon concentration and temperature, *Scripta METALLURGICA et MATERIALIA*, 29: 1011-1016.
- Richter F. (1983), *Physikalische Eigenschaften von Stählen und ihre Temperaturabhängigkeit*, Verlag Stahleisen GmbH, Düsseldorf.
- Winter K.M. (2011), Independently controlled Carbon and Nitrogen Potential. A new approach to Carbonitriding processes, Proc. 26<sup>th</sup> Heat Treating Society Conference, Detroit, USA: 9-16.
- Young R. A. (1993), *The Rietveld Method*, IUCr Book Series, Oxford University Press, :1-39.